

# Effect of Melt Thermal Treatment on Eutectic Silicon Particles Characteristics in Cast Al-Si-Mg Alloys

S.A. Al Kahtani

<sup>1</sup>Industrial Engineering Program, Mechanical Engineering Department, College of Engineering,  
Salman Bin Abdulaziz University, Al Kharj, Saudi Arabia  
salqahtany@hotmail.com

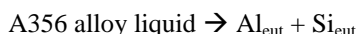
**Abstract-** A new means of obtaining fine Si particles is through the use of a melt thermal treatment (MTT), where the mixing of low and high temperature alloy melts produces a fine Si structure. Modification is achieved by nuclei resulting from the degeneration of large atom clusters and some refractory solids in the low temperature melt when it is heated by the high temperature melt. This is a relatively recent technique which demonstrates promise as an alternative to Sr-modification, as it requires no element addition, thus reducing the risk of increased porosity normally associated with the addition of strontium to the melt. The use of melt superheat is also found to produce refinement of the eutectic Si structure. In this case, the high melt temperature assists in the degeneration of atom clusters, providing more nuclei for  $\alpha$ -Al dendrite formation, and a resulting refinement of the microstructure.

**Keywords-** Melt Thermal Treatment; Melt Superheat; Sr Modification Eutectic Si Particle Characteristics

## I. INTRODUCTION

The Al-Si-Mg alloy system has excellent casting characteristics, weldability, pressure tightness and corrosion resistance. With heat treatment, Al-Si-Mg alloys can provide a wide range of physical and mechanical properties. Such alloys are commonly used in automobile components such as engine blocks and wheels.

Among Al-Si-Mg alloys, A356.2 is a commercially popular alloy, known for its excellent mechanical properties and high strength-to-weight ratio. The use of a heat treatment consisting of, for example, a solution heat treatment at 540°C, followed by quenching and natural or artificial aging, allows for the formation of interdendritic non-equilibrium precipitates of  $Mg_2Si$  and changes in the Si particle characteristics [1, 2]. The A356.2 alloy contains 0.3%-0.45% Mg which can induce age hardening through the precipitation of  $Mg_2Si$ ; the higher the Mg content, the more the age hardening that can be achieved. During solidification of A356, as the melt temperature drops to 577.6°C (widely accepted as Al-Si eutectic temperature [3]), the Al-Si eutectic reaction takes place. This reaction occurs at 577.6°C, at a Si level of ~12%.



As can be seen, the liquid alloy is completely transformed to nearly pure Si and Al in solid solution. The solid solution of Al can contain up to 1.5 wt% Si at the eutectic temperature. However, the solubility of silicon in aluminum decreases with temperature, e.g., to 0.05 wt% at 300°C [4]. The Al-Si eutectic nucleates on the primary aluminum dendrites and grows into the interdendritic regions during the reaction. From the Al-Si binary phase diagram, it can be estimated that A356 (Al-7%Si-0.4%) alloy contains approximately 50% Al-Si eutectic.

The Si particle characteristics, especially the morphology, also influence the mechanical properties, where a change from an acicular to a fibrous morphology improves the properties, in particular, ductility. In this regard, molten metal processing (melt treatment) and casting techniques, as well as the type of heat treatment applied are the factors by which the form and size of the Si particles can be controlled [1]. Several elements are known to cause eutectic Si modification. Group IA and Group IIA elements of the Periodic Table, i.e. rare earth elements (e.g. La, Ce), As, Sb, Se and Cd have all been reported to exert a modification effect [5]. However, only sodium (Na), strontium (Sr) and antimony (Sb) have ever been used. Among them, Sb, due to its toxic effects, is not used in North America. Due to its low boiling point, the 'fading' or poor retention of Na in the melt once added, leaves Sr as the modifier of choice in present-day foundry operations.

Melt thermal treatment (MTT), first reported by Valanbun in the 1960's [6], appears to be a promising alternative to chemical modification in that it can reduce some of the latter's negative effects such as increased porosity. Analysis of MTT processed Al-Si alloy castings shows that the resulting microstructure is significantly refined, leading to a considerable increase in the tensile strength-to-elongation ratio.

The present research work was undertaken to investigate various means of obtaining a fine eutectic Si in the as-cast microstructure of the A356.2 alloy via the effects of cooling rate, Sr-modification, super heating, and melt thermal treatment.

## II. EXPERIMENTAL PROCEDURE

The A356.2 casting alloy was received in the form of 12.5 kg ingots. Table 1 lists the chemical composition of the as-

received ingots. The A356.2 ingots were cut into smaller pieces, cleaned, dried and melted in a 7-kg capacity SiC crucible, using an electrical resistance furnace. The melting temperature was kept at  $750^{\circ}\text{C} \pm 5^{\circ}\text{C}$ .

TABLE 1 CHEMICAL COMPOSITION OF AS-RECEIVED A356.2 INGOT (WT.%)

Ingot Type	Si	Mg	Fe	Cu	Mn	Zn	Ti	Pb	Al
A356.2	6.78	0.33	0.11	0.02	0.04	0.04	0.08	0.03	bal.

During the preparation of the castings corresponding to various melt treatments and conditions, 6-kg charges of A356.2 alloy were melted in each case. The melts, per 6-kg charge of metal, were grain refined, using 55 g of Al-5%Ti-1%B master alloy. Degassing was carried out using pure dry argon, injected into the melt by means of a graphite rotary degassing impeller. The degassing time/speed were kept constant at 30 min/150 rpm.

For the preparation of the Sr-modified (SrM) castings, the melt was modified using a Al-10%Sr master alloy after degassing, where 12 g of the master alloy was added (to the 6 kg charge) to provide a Sr level of 200 ppm. The melt was stirred carefully and held for ~20 min to ensure proper dissolution of Sr into the melt, followed by another 10 min of degassing prior to pouring. Table 2 summarizes the details corresponding to all of the prepared castings.

TABLE 2 DETAILS OF THE VARIOUS A356.2 END-CHILL CASTINGS PREPARED FOR THE PRESENT WORK

Casting Type	Melt Condition /Treatment	Charge	Additions to Charge	Melt/Pouring Temperature	No. of Castings Prepared
NM	As-received (non-modified) + grain refined	6kg	55g Al-5% Ti-1% B	$750^{\circ}\text{C}$	10
SrM	Grain refined + Sr-modified	6kg	55g Al-5% Ti-1% B 12g Al-10% Sr	$750^{\circ}\text{C}$	10
SH	Grain refined + Superheated ( $900^{\circ}\text{C}$ )	6kg	55g Al-5% Ti-1% B	$900^{\circ}\text{C}$	6
MTT	MTT process-treated Non-modified + grain refined LTM ( $600^{\circ}\text{C}$ ) HTM ( $900^{\circ}\text{C}$ )	6kg  (2kg) (4kg)	  55g Al-5% Ti-1% B	  $670^{\circ}\text{C}$	  6
SrMTT	MTT process-treated Grain refined + Sr modified LTM ( $600^{\circ}\text{C}$ ) HTM ( $900^{\circ}\text{C}$ )	6kg  (2kg) (4kg)	  55g Al-5% Ti-1% B 3g Al-10% Sr	  $670^{\circ}\text{C}$	  6

For the preparation of castings using superheated (SH) melts, the melt temperature was increased to  $900^{\circ}\text{C}$ , with the melt being held at this temperature for 20 min and then poured into the mold. Castings were prepared using a rectangular end-chilled mold. The four walls of the mold are made of refractory material, while the bottom consists of a water-chilled copper base, to provide directional solidification. This type of mold is designed to provide a range of cooling rates along the height of the casting above the chill end.

The mold was preheated at  $225^{\circ}\text{C}$  for at least 2-3 hours to remove all moisture. The molten metal was poured into the mold through ceramic foam filter discs fitted into the riser to avoid oxides and inclusions from entering the mold. The water (circulating in the copper chill) was turned on as soon as the liquid metal had filled the mold to 3 cm. Such an arrangement produced ingot blocks with solidification rates that decreased with increasing distance from the chill end, giving microstructures that exhibited secondary dendrite arm spacings (DAS) from 15 to  $85\text{ }\mu\text{m}$  along the height of the cast block.

For the preparation of castings using the MTT process, a 6-kg charge of A356.2 alloy was melted at  $750^{\circ}\text{C}$ , grain refined and degassed using the same procedures already described. Following this, 4 kg of the melt was transferred to the other furnace, already preheated to  $750^{\circ}\text{C}$ . The temperature of the first furnace was then lowered to  $600^{\circ}\text{C}$ , while that of the second was increased to  $900^{\circ}\text{C}$ . The corresponding low temperature melt (LTM) and high temperature melt (HTM) were held at their respective temperatures for 20 min, followed by 15 min of degassing. The HTM melt was then poured into the LTM melt, and the mixture was stirred carefully, followed by pouring into the end-chilled mold.

For the preparation of Sr-modified (and grain-refined) castings using the MTT process (SrMTT), the same procedure was followed, except that the initial 6-kg melt was modified using 10 g of Al-10% Sr master alloy to give a Sr level of 100 ppm, followed by degassing for another 10-15 min. Following this, 4 kg of the modified melt was transferred to the other furnace and the same procedures were followed of preparing the LTM and HTM melts, mixing them and then pouring the melt into the end-chilled mold.

The end-chill castings that were prepared corresponding to the various melt treatments and processes were sectioned to obtain blanks and, subsequently, samples for solution heat treatment, metallography and tensile testing. Fig. 1 shows a schematic diagram of an end-chill casting.

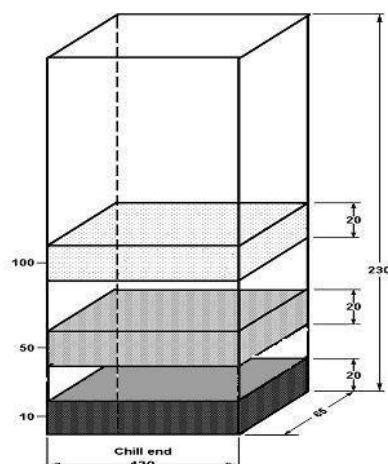


Fig. 1 Schematic diagram of the end-chill casting (all dimensions in mm)

Three specimen blanks were sectioned from each of the prepared castings, at heights of 10, 50 and 100 mm from the chill end, and corresponding to average DAS of 37, 62 and 78  $\mu\text{m}$  respectively as shown in Table 3.

TABLE 3 SDAS VALUES OBTAINED AT VARIOUS LEVELS OF THE END-CHILL CASTING

Level #	Distance From the Chill End (mm)	SDAS ( $\mu\text{m}$ )
1	10	37
2	50	62
3	100	78

Each of the three specimen blanks obtained per casting was further sectioned into 21 parts and numbered, following the sequence shown in Fig. 2.

1	2	3	4	5	6	7
8	9	10	11	12	13	14
15	16	17	18	19	20	21

Fig. 2 Sectioning of specimen blank for sample preparation (for solution heat treatment and metallography)

The DAS values were determined by measuring the secondary dendrite arm spacings from the corresponding metallography samples using an optical microscope-image analyzer system. At least 40 measurements were made for each sample and the average value was taken to represent the DAS value for the corresponding level. A quantitative evaluation of the eutectic Si particle characteristics was carried out using image analysis. From these measurements, the average value and standard deviation were obtained in each case.

### III. RESULTS AND DISCUSSION

The optical micrographs taken from the various A356.2 alloy casting types are presented in this section. For simplicity, the five casting types studied will be referred to by their casting codes as shown in Table 3. Fig. 3 show the eutectic Si particle characteristics displayed by the A356.2 alloy castings corresponding to the five casting types. Each figure displays the microstructures obtained at levels 1, 2 and 3 of each casting, corresponding to DAS of 37  $\mu\text{m}$ , 62  $\mu\text{m}$  and 78  $\mu\text{m}$ , respectively.

As can be seen from Fig. 3, the non-modified (NM) casting displays the typical acicular Si particles. Some amount of refinement due to cooling rate is observed in Fig. 3(a), compared to Figs. 3(b) and (c). In effect, the dendrite arm spacings of Levels 2 and 3 are not that far apart and hence their microstructures would be more similar than different, particularly when compared to that of Level 1, with a dendrite arm spacing almost half of the others.

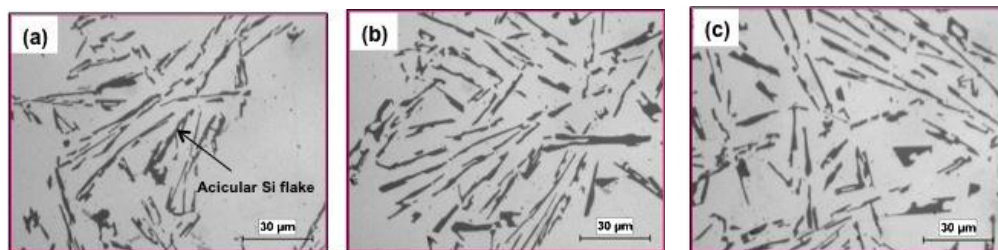


Fig. 3 Optical micrographs showing the eutectic Si particle characteristics observed in as-cast samples of the NM (non-modified) A356.2 alloy casting: (a) level 1, DAS 37  $\mu\text{m}$ ; (b) level 2, DAS 62  $\mu\text{m}$ ; (c) level 3, DAS 78  $\mu\text{m}$

Tolui and Hellawell [7] and Hogan and Song [8] have reported that the Si interparticle spacing decreases with increase in cooling rate and vice versa. This is evidenced to some extent in Fig. 3. With the introduction of 200 ppm Sr to the melt, the eutectic Si particles are completely transformed from long, acicular plates to well-modified fibrous particles. The very fine particle size results in a significant increase in the Si particle density. The observation of a well-modified eutectic structure in A356.2 alloys with Sr addition is well reported [9, 10].

In Fig. 4, while the eutectic Si regions are well modified, a certain number of unmodified or partially modified Si particles are always observed close to the  $\alpha$ -Al dendrites. This phenomenon is a result of the distribution of Si concentration within the  $\alpha$ -Al dendrites. The areas close to the dendrites contain higher Si concentrations, requiring more strontium to become fully modified. However, due to the high cooling rate produced by the end-chill mold, there is less time for the strontium to be distributed to these areas and thus there is not enough strontium available to fully modify the eutectic Si particles, leaving them partially modified or unmodified.

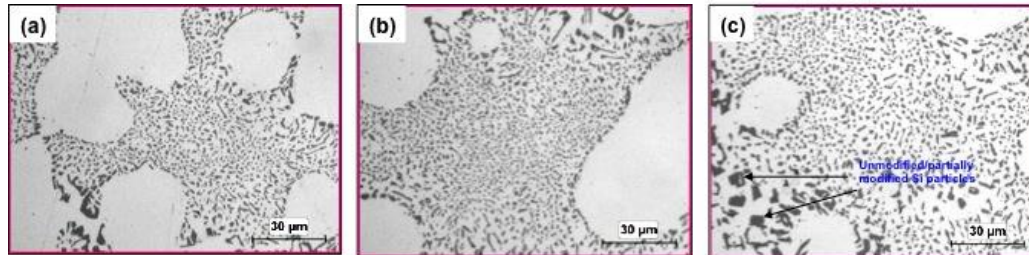


Fig. 4 Optical micrographs showing the eutectic Si particle characteristics observed in as-cast samples of the SrM (200 ppm Sr-modified) A356.2 alloy casting: (a) level 1, DAS 37  $\mu\text{m}$ ; (b) level 2, DAS 62  $\mu\text{m}$ ; (c) level 3, DAS 78  $\mu\text{m}$

Fig. 5 shows that superheating of the melt has a remarkable refining effect on the eutectic Si in A356.2 alloy. This effect can be attributed to the dissolution of atom clusters present in the melt at the superheat temperature. According to Pople and Sidorov [11], if the superheat temperature is high enough for the atom clusters to dissolve fully in the melt, the cooling rate should have no effect on the eutectic Si particle characteristics in the microstructure. However, by comparing Figs. 5(a), (b) and (c), it can be seen that the size of the eutectic Si particles increases somewhat as the cooling rate decreases, so it can be concluded that the 900°C melt superheat temperature used in the present study is not high enough to achieve the same results. Therefore, in the present case, the microstructure of the eutectic Si particles is determined by both the superheat temperature and the cooling rate [12].

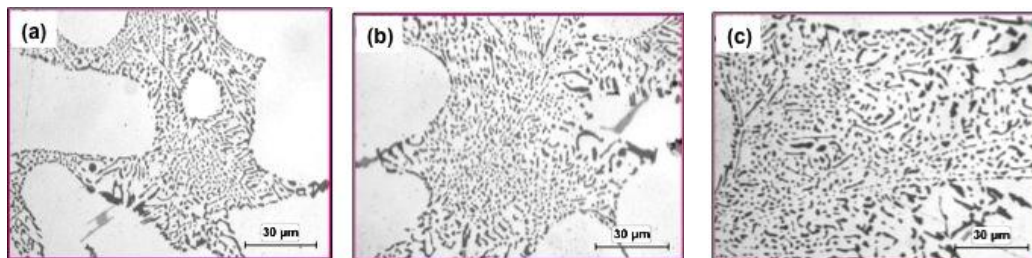


Fig. 5 Optical micrographs showing the eutectic Si particle characteristics observed in as-cast samples of the SH (superheated) A356.2 alloy casting: (a) level 1, DAS 37  $\mu\text{m}$ ; (b) level 2, DAS 62  $\mu\text{m}$ ; (c) level 3, DAS 78  $\mu\text{m}$

Figs. 6 and 7 compare the effects of MTT on the microstructures of castings obtained from unmodified and Sr-modified A356.2 alloy melts, respectively. Although the eutectic Si particles are refined in the MTT-processed casting of the unmodified alloy, they still retain their acicular morphology. This observation was also reported by Wang *et al.* [13]. A combination of Sr-modification and the MTT process results in very fine eutectic Si regions, where the acicular, larger-sized Si particles that were observed at the edges of the  $\alpha$ -Al dendrites in Fig. 4 (for the Sr-modified alloy) appear to have been minimized considerably in the SrMTT casting (Fig. 7).

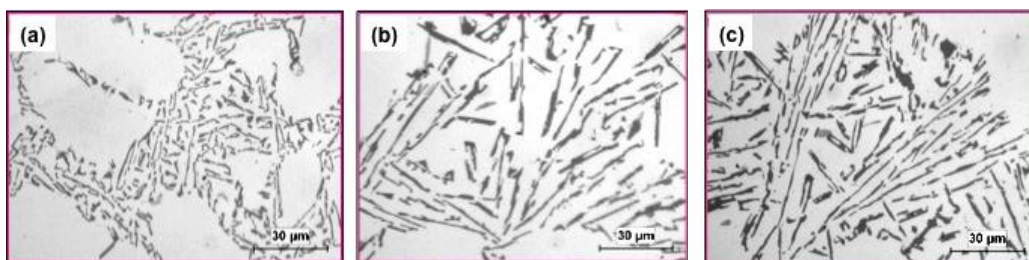


Fig. 6 Optical micrographs showing the eutectic Si particle characteristics observed in as-cast samples of the MTT processed A356.2 alloy casting: (a) level 1, DAS 37  $\mu\text{m}$ ; (b) level 2, DAS 62  $\mu\text{m}$ ; (c) level 3, DAS 78  $\mu\text{m}$



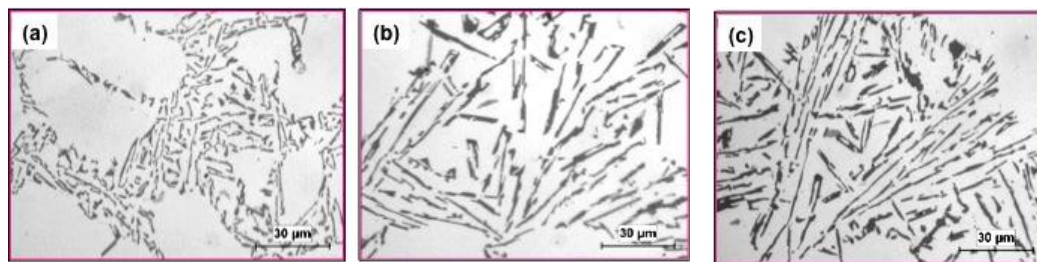


Fig. 7 Optical micrographs showing the eutectic Si particle characteristics observed in as-cast samples of the SrMTT (100 ppm Sr-modified + MTT processed) A356.2 alloy casting: (a) level 1, DAS 37  $\mu\text{m}$ ; (b) level 2, DAS 62  $\mu\text{m}$ ; (c) level 3, DAS 78  $\mu\text{m}$

In this regard, it should be mentioned that in the MTT casting obtained from the non-modified A356.2 alloy, the refining (or modifying) effect was not homogeneous over the sample surface. As Fig. 8 shows, the eutectic Si particles in (a) are comparatively well refined, while those in (b) are a mix of refined and unrefined Si particles. Both micrographs were taken from the MTT casting-level 1 sample. This irregularity in modification may be caused by the inhomogeneous transfer of thermal energy when the LTM and HTM melts are mixed. On account of this, atom clusters that are not broken into smaller nuclei will eventually result in the formation of larger Si particles upon solidification.

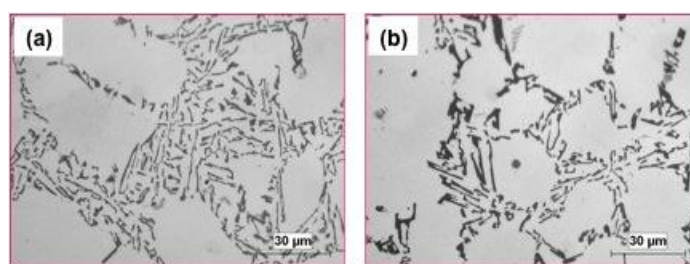


Fig. 8 Optical micrographs corresponding to two fields of observation in the MTT casting-level 1 sample, showing (a) well-refined, and (b) inhomogeneously refined eutectic Si regions

As previously mentioned, there appears to be very little literature that reports on the MTT process in the context of the modification of Al-Si alloys. The present study extended the work of Wang *et al* [13], to investigate the combined effect of Sr addition and the MTT process on the modification effect in the A356.2 alloy by modifying the alloy melt with 100 ppm Sr before subjecting it to the melt thermal treatment process. As Fig. 7 shows, the combination of Sr-modification and MTT process produces the best results as far as obtaining a well-modified eutectic is concerned. The uniformity of the eutectic Si particle size throughout the eutectic regions is remarkable. Compared to the 200 ppm SrM case hardly any large Si particles are observed at the periphery of the  $\alpha$ -Al dendrites.

It should be mentioned here that, for the SrMTT casting, only 100 ppm Sr was used, to determine if a less amount of Sr than that usually employed for obtaining a well-modified eutectic structure in Al-Si alloys would suffice to obtain the same level of modification after the MTT process was carried out. A quantification of the eutectic Si particle characteristics using image analysis showed that the SrMTT casting samples provided the smallest Si particle sizes, followed by the SrM and then the SH casting samples. The level of modification observed in the different A356.2 alloy castings corresponding to the NM, SrM, 900°C SH, MTT processed and SrMTT processed castings are compared in Fig. 9 for samples obtained from Levels 1 and 3 of each casting, corresponding to DAS values of 37  $\mu\text{m}$  and 78  $\mu\text{m}$ , respectively.

As can be seen, well-modified fibrous Si particles are produced with SrM, SH and SrMTT processes, the latter producing the finest particles, while the use of the MTT process alone is seen to only refine the Si particles but not change their acicular morphology. The effect of cooling rate is apparent for the MTT-processed samples (Figs. 9(g) and 9(h)), and also evident to some extent in the NM, SrM and SH samples. The extremely fine Si particles in the case of the SrMTT casting render it difficult to distinguish the effect of cooling rate when comparing Figs. 9(i) and 9(j).

The effect of cooling rate on the Si particle characteristics in Al-Si alloys has been investigated by many researchers [11-14]. In the present study, the A356.2 alloy melts subjected to different modification methods were cast into end-chilled molds that provided a range of cooling rates in the same casting, along the height of the casting block. Three cooling rates were selected for study, at heights or levels of 10, 50 and 100 mm above the chill end and corresponding to DAS values of 37, 62 and 78  $\mu\text{m}$ , respectively. As the A356.2 alloy melts were modified before being cast, in examining the effect of cooling rate, the effects of the modification method used in each case would also be incorporated automatically.

Table 4 summarizes the results of the eutectic Si particle characteristics obtained for different samples in the as-cast condition. It can be seen that the cooling rate has a moderate to significant influence on the Si particle size in that the particle size increases as the cooling rate is decreased. The moderate effect is observed in the case of the non-modified alloy casting, where a gradual increase in the average Si particle area and length values is observed from Level 1 to Level 3. In comparison, the other four (modified) castings show a significant influence of the cooling rate, although this may not be that evident in the

case of the SrMTT casting samples, compared to the MTT casting samples, on account of the very fine particle sizes obtained in the former. Similar results were reported by Mancheva *et al.* [14] who observed that the average Si particle area in AlSi7Mg castings improved from 0.9 to 0.4  $\mu\text{m}^2$  when the cooling rate was increased from 14.8 to 72.4 K/s.

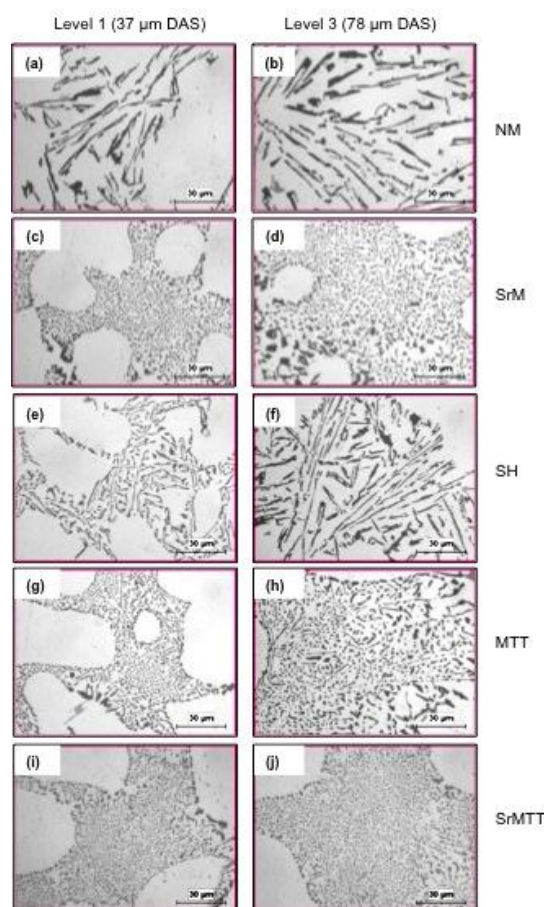


Fig. 9 Comparison of modification in different A356.2 alloy samples obtained from: (a, b) NM, (c, d) SrM, (e, f) SH, (g, h) MTT, and (i, j) SrMTT castings in the as-cast condition, and corresponding to levels 1 and 3 in each case

TABLE 4 EUTECTIC SI PARTICLE CHARACTERISTICS OF DIFFERENT CASTING SAMPLES OBTAINED IN THE AS-CAST CONDITION

Casting Type	Area ( $\mu\text{m}^2$ )						Length ( $\mu\text{m}$ )					
	Level 1		Level 2		Level 3		Level 1		Level 2		Level 3	
	(DAS 37 $\mu\text{m}$ )		(DAS 62 $\mu\text{m}$ )		(DAS 78 $\mu\text{m}$ )		(DAS 37 $\mu\text{m}$ )		(DAS 62 $\mu\text{m}$ )		(DAS 78 $\mu\text{m}$ )	
	Avg.	S.D.	Avg.	S.D.	Avg.	S.D.	Avg.	S.D.	Avg.	S.D.	Avg.	S.D.
NM	25.33	28.46	26.32	29.11	27.32	30.09	11.96	11.39	13.57	12.85	14.62	13.93
SrM	1.16	1.94	2.82	4.09	3.08	4.26	1.57	1.36	2.36	1.91	2.48	2.03
SH	1.62	3.37	2.8	4.45	4.4	6.2	1.94	2.04	2.62	2.54	3.29	2.96
MTT	2.94	4.56	5.04	8.48	8.98	12.95	3.2	3.21	4.42	5.11	6.11	6.22
SrMTT	0.94	1.85	1.38	2.44	1.53	2.7	1.4	1.28	1.74	1.6	1.87	1.72
Casting Type	Roundness (%)						Aspect Ratio					
	Level 1		Level 2		Level 3		Level 1		Level 2		Level 3	
	(DAS 37 $\mu\text{m}$ )		(DAS 62 $\mu\text{m}$ )		(DAS 78 $\mu\text{m}$ )		(DAS 37 $\mu\text{m}$ )		(DAS 62 $\mu\text{m}$ )		(DAS 78 $\mu\text{m}$ )	
	Avg.	S.D.	Avg.	S.D.	Avg.	S.D.	Avg.	S.D.	Avg.	S.D.	Avg.	S.D.
NM	45.24	28.42	42.82	28.48	40.8	27.24	2.64	1.37	3.13	1.74	3.3	1.83
SrM	75.24	20.64	77.23	21.45	77.23	21.23	1.81	0.66	1.53	0.37	1.65	0.55
SH	74.76	22.84	74.78	23.2	73.43	23.77	1.85	0.78	1.79	0.75	1.79	0.72
MTT	56.96	27.34	55.26	29.51	51.16	29.97	2.51	1.33	2.91	1.62	2.76	1.52
SrMTT	78.87	20.35	77.32	20.87	75.81	21.48	1.81	0.67	1.83	0.69	1.87	0.72

While cooling rate affects the Si particle size, Fig. 10 shows that the shape of the Si particles is not affected by the change in cooling rate. Both the average roundness and average aspect ratio values (and their standard deviations) remain more or less the same from one level to the next. This is to be expected, since these parameters relate to the morphology, rather than the size, of the Si particles, with roundness values close to 100 and an aspect ratio of 1.0 (representing completely spherical particles). As can be seen, the acicular particles of the non-modified alloy display low roundness values (<50%) and high aspect ratios (2.6-3.3), whereas the SrM, SH and SrMTT castings have much higher roundness values (75–77%) and comparatively lower aspect ratios (~1.8). The standard deviations obtained for these two parameters are also approximately similar for the SrM, SH and SrMTT castings (roundness value: ~20 and aspect ratio: ~0.7, respectively), indicating that these parameters are influenced by the modification process rather than the cooling rate.

In contrast to the modified castings discussed above, the MTT casting samples exhibit roundness and aspect ratio values that are comparable to, but somewhat lower than, those obtained for the non-modified alloys, indicating that the Si particles, although refined, still retain their acicular morphology. Also, the standard deviations observed for these two parameters for the MTT and NM casting samples are higher (~28 and ~1.35-1.7, respectively), compared to those noted for the SrM, SH and SrMTT castings.

Similar results corresponding to the NM and SrM castings in the present work were obtained by Paray and Gruzleski [15] in their studies on non-modified and Sr-modified A356 alloys. Their experimental results showed that for A356 alloy castings, drawn from a permanent mold, the average Si particle area was refined from  $3.81 \mu\text{m}^2$  in the non-modified alloy casting to  $0.24 \mu\text{m}^2$  in the 200 ppm Sr-modified alloy casting, and the average aspect ratio improved from 2.17 to 1.74.

With respect to the average and standard deviation values listed in Table 4, it must be noted that due to the wide range of Si particle sizes observed, it is expected that the standard deviation will be of the order of or higher than the average value. The particle size distribution plotted by the image analyzer system provides a range of Si particle sizes and the corresponding particle counts. It is found that the maximum particle count generally corresponds to the particle size range which includes or lies close to the average value calculated by the system. In other words, the average values *do* reflect the overall modification effect obtained from casting type to casting type.

The results of Table 4 have been presented in Figs. 10-13 in the form of histograms, which facilitate in distinguishing the effect of cooling rate (or dendrite arm spacing), and that of the modification process on the Si particle characteristics. In general, the Si particle area and length of the MTT casting appear to be the most sensitive to the cooling rate, followed by the NM and SH castings (Figs. 10 and 11). In the SrM casting, an improvement due to cooling rate is evidenced mainly at the cooling rate corresponding to the lowest DAS (37  $\mu\text{m}$ ). The particle size remains constant at DAS levels of 62  $\mu\text{m}$  and above.

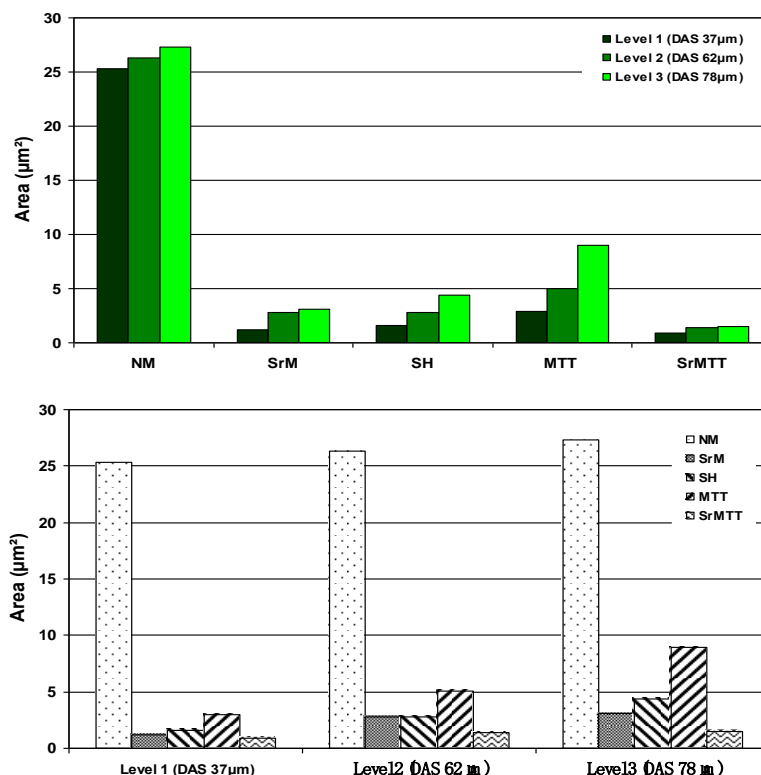


Fig. 10 Average Si particle area obtained for as-cast samples taken from different A356.2 alloy castings/levels, showing the effect of (i) cooling rate, casting level/DAS (top chart) and (ii) modification process, casting type (bottom chart)

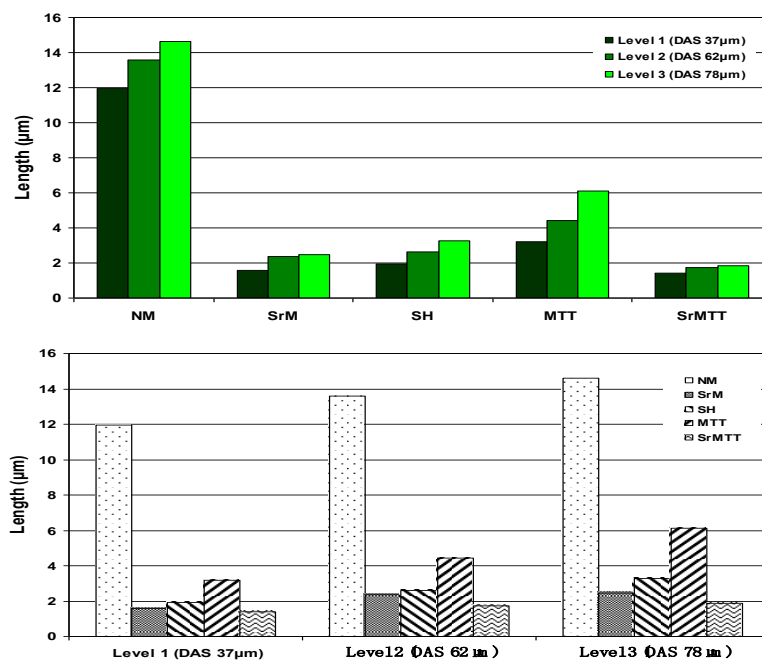


Fig. 11 Average Si particle length obtained for as-cast samples taken from different A356.2 alloy castings/levels, showing the effect of (i) cooling rate, casting level/DAS (top chart) and (ii) modification process, casting type (bottom chart)

Compared to all these casting types, the SrMTT casting shows the best results in that not only the Si particle sizes are the smallest among all castings, but also these values remain approximately constant over the range of cooling rates studied. This has a great significance from an application point of view. Often, cast parts contain sections of varying thickness, and in such cases, the use of a SrMTT processed Al-Si alloy melt in casting would ensure a relatively uniform eutectic Si particle size throughout the casting, and therefore, guarantee its overall properties.

With respect to the roundness parameter, the best results are obtained with the SrMTT casting which displays consistently high roundness values, with a very small influence due to cooling rate. The aspect ratios, however, are similar to those obtained for the SH and SrM castings. The moderate amount of refinement in the Si particle morphology in the MTT casting compared to the NM casting can also be observed from Figs. 12 and 13.

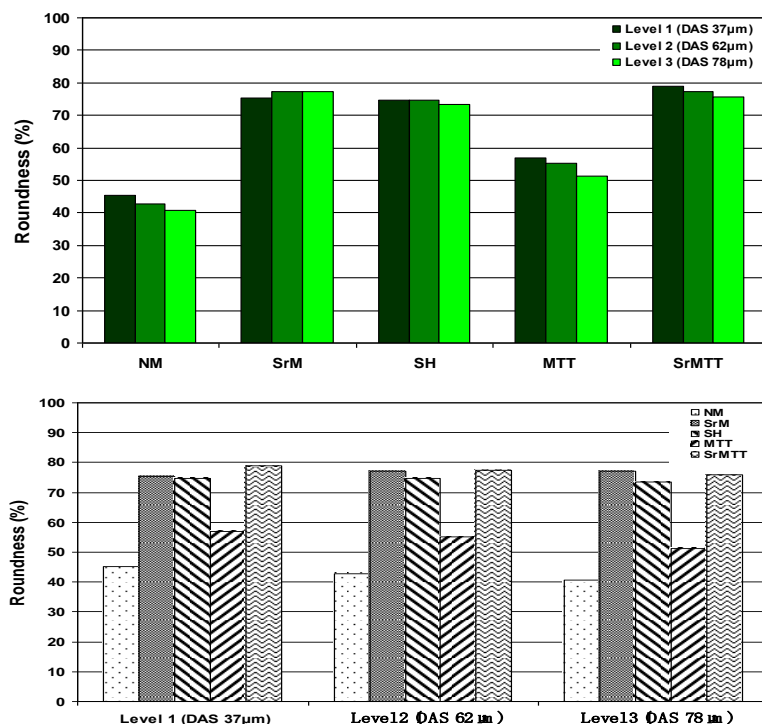


Fig. 12 Average Si particle roundness obtained for as-cast samples taken from different A356.2 alloy castings/levels, showing the effect of: (i) cooling rate, casting level/DAS (top chart) and (ii) modification process, casting type (bottom chart)



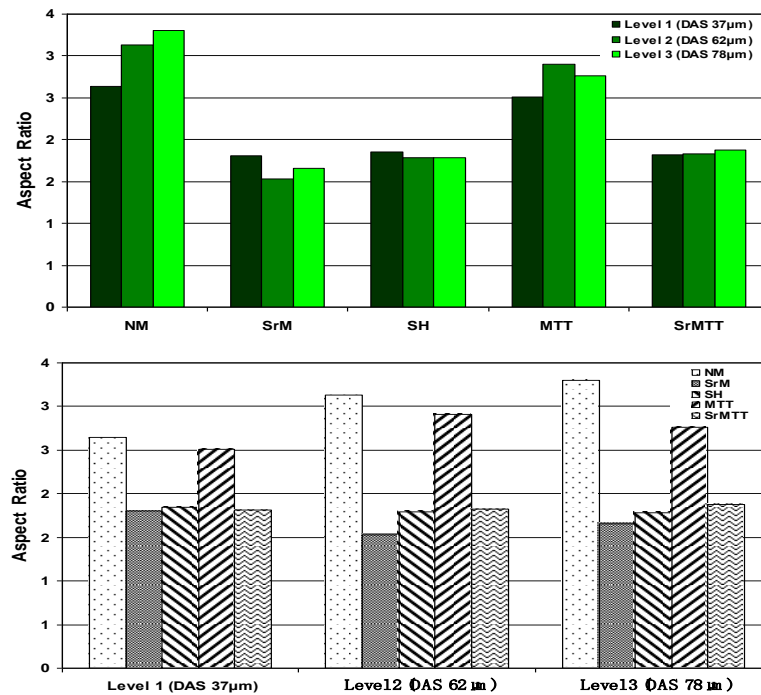


Fig. 13 Average Si particle aspect ratio obtained for as-cast samples taken from different A356.2 alloy castings/levels, showing the effect of: (i) cooling rate, casting level/DAS (top chart) and (ii) modification process, casting type (bottom chart)

The various modification methods applied to A356.2 alloy in the present work were used to determine which would produce a well-modified, fibrous eutectic structure, *viz.* those that reduced the Si particle size and aspect ratio to a minimum and increased the roundness to a maximum. Theoretically, spherical particles would have a roundness value of ~100% and an aspect ratio of 1.

To compare the efficiencies of the different modification methods, the Si particle characteristics obtained for the SrM, SH, MTT and SrMTT casting samples were compared with those obtained for the NM casting in terms of the percentage *decrease* in the area and length parameters, the percentage *increase* in the roundness, and the percentage *decrease* in the aspect ratio, as shown in Tables 5 and 6. The values in the parentheses in the row for the NM casting in both tables represent the actual values obtained for each parameter at the corresponding level. Those listed in the other rows provide the percentage changes in the four parameters (area, length, roundness and aspect ratio) observed in the other casting samples calculated in terms of the NM values in parentheses. The actual values are given in Table 4.

TABLE 5 CHANGE IN SI PARTICLE SIZE ACHIEVED FOR DIFFERENT CASTING TYPES IN COMPARISON TO THE NON-MODIFIED CASTING

Casting Type	Percentage Change in Si Particle Size					
	% Decrease in Area ( $\mu\text{m}^2$ )			% Decrease in Length ( $\mu\text{m}$ )		
	Level 1 (10mm)	Level 2 (50mm)	Level 3 (100mm)	Level 1 (10mm)	Level 2 (50mm)	Level 3 (100mm)
NM	(25.33)	(26.32)	(27.32)	(11.96)	(13.57)	(14.62)
SrM	95.4%	89.3%	88.7%	86.9%	82.6%	83.1%
SH	93.6%	89.4%	83.9%	83.4%	80.7%	77.5%
MTT	88.4%	80.9%	67.1%	73.3%	67.5%	58.2%
SrMTT	96.3%	94.7%	94.4%	88.1%	87.2%	87.2%

Note: levels 1, 2 and 3 correspond to DASs of 37, 62 and 78  $\mu\text{m}$ , respectively

TABLE 6 CHANGE IN SI PARTICLE SHAPE ACHIEVED FOR DIFFERENT CASTING TYPES IN COMPARISON TO THE NON-MODIFIED CASTING

Casting Type	Percentage Change in Si Particle Shape					
	% Increase in Roundness			% Decrease in Aspect Ratio		
	Level 1 (10mm)	Level 2 (50mm)	Level 3 (100mm)	Level 1 (10mm)	Level 2 (50mm)	Level 3 (100mm)
NM	(45.24)	(42.82)	(40.80)	(2.64)	(3.13)	(3.30)
SrM	66.31%	80.36%	89.29%	31.44%	51.12%	50.00%
SH	65.25%	74.64%	79.98%	29.92%	42.81%	45.76%
MTT	25.91%	29.05%	25.39%	4.92%	7.03%	16.36%
SrMTT	74.34%	80.57%	85.81%	31.44%	41.53%	43.33%

Note: levels 1, 2 and 3 correspond to DASs of 37, 62 and 78  $\mu\text{m}$ , respectively

In their study of the effect of Sr modification in A356.2 alloy, Paray and Gruzleski [15] found that strontium affects not only the size and morphology of the eutectic Si particles, but also the particle size and morphology distribution. Their conclusions, which correspond to the NM and SrM castings in the present work, can also be extended to the SH, MTT and SrMTT castings as well, where the standard deviation obtained for each parameter measured can be used to estimate the structural uniformity of the eutectic Si particles in A356.2 alloy. The narrower the standard deviation is, the more homogeneous the Si particle size and morphology distribution are. In other words, the higher the degree of modification achieved.

#### IV. CONCLUSIONS

1. The acicular eutectic silicon observed in non-modified A356.2 alloy can be modified using various means such as Sr-modification (SrM), superheat melt (SH), melt thermal treatment (MTT) and a combination of Sr-modification and MTT (SrMTT). Strontium modification, superheat and Sr-modified-MTT processed castings provide fine eutectic Si particles, the SrMTT process giving the best modification results. The MTT process alone provides a moderate amount of modification.

2. Compared to all casting types, the SrMTT casting shows the best results in that not only the Si particle sizes are the smallest among all the castings, but these values remain approximately constant over the ranges of cooling rates studied. This has great significance from an application point of view, as cast parts often contain sections of ranging thickness, and the use of a SrMTT processed Al-Si alloy melt would ensure a relatively uniform eutectic Si particle size throughout the casting, and hence, guarantee its overall properties.

3. Both size and morphology of the eutectic silicon particles are affected by the modification process used. The SrM, SH and SrMTT castings show well modified fibrous Si particles, whereas the MTT casting exhibits Si particles that, although refined to a certain extent, still retain their acicular morphology.

4. Cooling rate affects the eutectic Si particle size in that a higher cooling rate produces finer Si particles. However, within the range of cooling rates provided by the end-chill mold used in this work, the cooling rate does not affect the morphology of the Si particles.

#### ACKNOWLEDGMENTS

The author would like to thank Prof. F.H. Samuel of the Université du Québec à Chicoutimi, Québec, Canada for all technical support and to Dr. Ehab Samuel of the National Research Council Canada - Aluminum Technology Center for editing the present research article.

#### REFERENCES

- [1] D. Apelian, S. Shivkumar and G. Sigworth: Fundamental Aspects of Heat Treatment of Cast Al-Si-Mg Alloys, *AFS Transactions*, **97**(1989), pp. 727-742.
- [2] S. Shivkumar, C. Keller and D. Apelian: Aging Behavior in Cast Al-Si-Mg Alloys, *AFS Transactions*, **98**(1990), pp. 905-911.
- [3] J. R. Davis (Editor): *Aluminum and aluminum alloys*, ASM International, Ohio, 1993, p. 627.
- [4] S. Shankar, Y. W. Riddle and M. M. Makhlof: Nucleation mechanism of the eutectic phases in aluminum-silicon hypoeutectic alloys, *Acta Materialia*, **52**(2004), pp. 4447-4460.
- [5] J. E. Gruzleski: The Art and Science of Modification: 25 Years of Progress, Silver Anniversary Paper, *AFS Transactions*, **100**(1992), pp. 673-683.
- [6] G. F. Valanbun:, Moscow, Mashgiz, 1965, p. 255.
- [7] B. Tolui and A. Hellawell: Phase separation and undercooling in an Al-Si eutecticalloy - The influence of freezing rate and temperature gradient, *Acta Metallurgical*, **24**(1976), pp. 565-573.
- [8] L. M. Hogan and H. Song: Interparticle spacings and undercoolings in Al-Si eutectic microstructures, *Metallurgical Transactions A*, **18A**(1970), pp. 235-237.
- [9] E. N. Pan, Y. C. Cherng, C. A. Li and H. S. Chiou: Roles of Sr and Sb on Silicon Modification of A356 Aluminum Alloys, *AFS Transactions*, **102**(1994), pp. 609-629.
- [10] P. E. Crosley and L. F. Mondolfo: The Modification of Aluminum-Silicon Alloys, *AFS Transactions*, **74**(1966), pp. 53-64.
- [11] P. S. Popel and V. E. Sidorov: Microheterogeneity of liquid metallic solutions and its influence on the structure and properties of rapidly quenched alloys, *Materials Science and Engineering A*, **226-228**(1997), pp. 237-244.
- [12] M. M. Tuttle and D. L. McLellan: Silicon Particle Characteristics in Al-Si-Mg Castings, *AFS Transactions*, **90**(1982), pp.13-23.
- [13] J. Wang, S. He, B. Sun, Y. Zhou, Q. Guo and M. Nishio: A356 alloy refined by melt thermal treatment, *International Journal of Cast Metals Research*, **14**(2001), pp. 165-168.
- [14] R. Lazarova-Mancheva, R. Kovacheva, G. Bachvarov and V. Manolov: Influence of the Cooling Rate on the Geometric Parameters of Eutectic Silicon in AlSi7Mg Castings, *Praksische Metallographie*, **39**(2002), pp. 28-35.
- [15] F. Paray and J. E. Gruzleski: Microstructure-mechanical property relationships in a 356 alloy. Part I: Microstructure, *Cast Metals*, **7**(1994), pp. 29-40.